Increased Efficiency of Shock Control Bumps for Buffet Onset Delay Due to Variable Camber

Jens Müller[1]([✉]), Andreas Waldmann[1], Andreas Goerttler[2],
Sven Christian Künnecke[3], and Thorsten Lutz[1]

[1] University of Stuttgart, Faculty 6, Institute of Aerodynamics and Gas Dynamics,
Pfaffenwaldring 21, 70569 Stuttgart, Germany
`jens.mueller@iag.uni-stuttgart.de`
[2] German Aerospace Center (DLR), Institute of Aerodynamics and Flow Technology,
Bunsenstraße 10, 37073 Göttingen, Germany
[3] DLR, Institute of Composite Structures and Adaptive Systems, Lilienthalplatz 7,
38108 Braunschweig, Germany

Abstract. Within this work, 2D numerical simulations are used to assess the potential of variable camber (VC) to increase the effectiveness in terms of buffet onset delay of shock control bumps on the airfoil of a HLFC wing. Since the bumps are restricted to the spoiler, positioning of the bump relative to the shock is not ideal, which limits the potential in shifting the transonic buffet boundary to higher lift coefficients. VC is used to move the shock towards the leading edge. This increases the capabilities of shock control bumps in moving buffet onset to higher lift coefficients values over a wide range of bump crest positions and bump heights. In addition, VC enables the usage of a structurally designed bump on a morphing spoiler, which is optimized for wave drag reduction without VC and can be used for buffet onset delay with VC applied.

Keywords: transonic buffet · shock control bumps · variable camber

1 Introduction

On conventional transport aircraft, airspeed and angle of attack are limited, among other things, by the occurrence of unsteady shock oscillation, the so-called transonic buffet. In transonic flow, the shock wave/boundary layer interaction leads to shock induced separation. The mutual interaction between separation and shock wave leads to a periodic movement of the shock together with a combination of reattachment and separation of the flow downstream from the shock. Further details on transonic buffet and current research are provided by Giannelis et al. [5]. Due to the unsteady aerodynamics and load fluctuations resulting from the buffet, a sufficient distance from the buffet limit must be ensured during flight [12]. An extension of the flight envelope to higher Mach numbers and angles of attack can be achieved by actively influencing the shock using shock control bumps (SCBs) [10]. SCBs were first introduced by Ashill et al. [1] as an effective

method for wave drag reduction in transonic flight. The bump's crest position should be located shortly downstream but close to the shock position to create a λ-shaped shock structure or, ideally, an isentropic compression. An overview of recent research regarding shock control bumps for wave drag reduction is provided in [3]. In terms of buffet onset delay, Birkemeyer et al. [2] found, that a bump located further downstream than for wave drag reduction is able to shift the buffet onset to higher lift coefficients c_L. Guidelines for bump design in terms of buffet onset delay are provided by Mayer et al. [10].

On today's commercial aircraft configurations, the available space for the integration of SCBs and their actuators is limited, which restricts the positioning of SCBs. Furthermore, the desirable use of a SCB for both drag reduction and buffet onset delay is very challenging as the design criteria regarding the position of bump and bump crest differ significantly. Both aspects can thus severely limit the effectiveness of SCBs in shifting the buffet boundary if the bump's crest position is too close to the shock location. If the position of the SCB is not optimal for buffet onset delay, there is a need to shift the location of the shock close to the buffet boundary to ensure an increase of the buffet c_L without violating geometric restrictions or reducing the effectiveness of the SCB to reduce wave drag in cruise flight. The shock position can be influenced, e.g. by static deflection of trailing edge flaps, which change the camber of the airfoil/wing (VC). Since VC has also an effect on the flow separation, it is possible to delay buffet onset as well. For supercritical airfoils, this is shown e.g. by Lee [9] and Despré et al. [4]. Werner [18] combines VC with the application of a SCB on a NLF wing in terms of an optimized wave drag reduction. It is shown that VC can be used to ensure an appropriate shock location relative to the SCB when the crest position of the SCB is limited to a small region of the wing. Richter et al. [13] demonstrate that when combining VC with a position fixed SCB drag reduction can be achieved over a broad range of Mach numbers. Hence, the question arises whether VC can also be used to increase the efficiency of SCBs in terms of buffet onset delay, when the SCB positioning is limited.

The current work is part of the LuFo project Move-IntegR, which focuses on the application of shock control bumps on a hybrid laminar flow control (HLFC) wing of a transonic airliner. It is based on the companion work by Waldmann et al. [17], where parameter studies of SCBs with a focus on buffet onset delay were performed. The aim of the present work is to increase the effectiveness of SCBs in terms of buffet onset delay by means of steady trailing edge flap deflections on a representative 2D airfoil of the HLFC wing. The SCBs are designed to fulfill the integration limitations by the aircraft design as well as considering structural feasibility of a morphing spoiler, which implements the bump shape. This limits the possible bump shapes and thus the SCB's effectiveness for buffet onset delay. The trailing edge flap deflection is used to change the camber of the airfoil in order to shift the shock to a desirable position in relation to the SCB. The impact of VC on the SCB performance is evaluated and the aerodynamic mechanisms are analyzed. Furthermore, it is examined whether VC enables the utilization of a structurally designed SCB on a morphing spoiler for buffet onset delay, which is without VC optimized for wave drag reduction in cruise flight.

## 2   Geometry and Simulation Methodology

The reference aircraft of the current work is the GBD-DLR-2 geometry provided by the DLR. This geometry is based on the Airbus XRF1 research aircraft, which was redesigned with HLFC within the HLFC-WIN project [16]. The aircraft contains fuselage, wing, nacelle, pylon, flap-track fairings, and vertical tail plane. From the engine mounting to the wing tip suction panels are installed in the leading edge area and the wing shape is modified to ensure laminar flow on the outer wing. The investigations within the work at hand are carried out on a 2D wing section extracted at $\eta = \frac{y}{0.5b} = 0.57$, which is located on spoiler 5. To account for the wing sweep of the 3D wing, the 2D airfoil geometry as well as the inflow conditions are transformed according to the cosine rule, see [12], with a sweep angle $\Lambda = 25°$. The reference cruise condition of the aircraft is $M_\infty = 0.85$ at $c_L = 0.5$. Details regarding the baseline flow and the 2D transformation are provided in [17]. Buffet onset for each bump/flap setting is determined from a lift polar with the $\Delta\alpha$ criterion described by Lawson et al. [8]. Details on the buffet determination and the corresponding linearization of the lift polar used within this work are provided in [17]. The lift polars are determined in stationary 2D RANS airfoil simulations utilizing the block structured, compressible, finite volume CFD solver FLOWer [14]. The Reynolds-Averaged Navier Stokes (RANS) equations are closed by the Spalart-Allmaras one-equation turbulence model. Each polar consists of 56 to 66 different angles of attack α with the inflow conditions equivalent to the 2D transformed cruise conditions of the reference aircraft. Due to the suction on the HLFC wing at this spanwise position, the laminar to turbulent transition is fixed at $x_{tr}/c = 48.4\%$ in all 2D simulations within this work. The simulation framework used in this work is described in the companion paper by Waldmann et al. [17]. In line with [17], the grid applied in the 2D CFD simulations is block structured and of C-H type. It is discretized with about 150 points located on the upper and lower side of the airfoil and point clustering in the vicinity of the shock and the spoiler. The grid topology is described by Mayer et al. [11].

Within the simulation framework, the bump shapes and the flap deflections are created by modifying the airfoil geometry prior to the mesh generation in Gridgen. The trailing edge flap of the GBD-DLR-2 geometry at $\eta = 57\%$ used for VC is located directly behind the spoiler at relative chord length $x/c > 85\%$. The flap deflection is realized by a rotation of the trailing edge around the hinge point M and an interpolation of this displacement vector to the rest of the flap depending on the x distance to the hinge point. The resulting flap deflection for $\delta = -2°$ and its orientation relative to a SCB is shown in Fig. 1.

To account for a robust parameter space, two different bump types, SCB1 and *StructConsid* (SC), are considered on the upper side of the airfoil based on the previous investigation by Waldmann et al. [17]. For each shape, bump crest position and bump height are varied while the geometrical extend is fixed to spoiler 5 ($70\% \leq x/c \leq 85\%$). This enables a structural integration via a morphing spoiler. The SCB1 shape is based on aerodynamic studies by Sommerer et al. [15]. It is designed for an optimized shock control but does not consider structural feasibil-
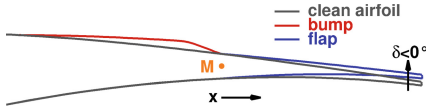
Fig. 1. Flap deflection
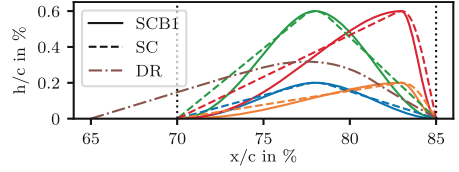
Fig. 2. Exemplary bump shape. Dotted vertical lines: spoiler start and end. Matching colors: similar x_{cr} and h_{cr}

ity. The SC bump shape, developed within the Move-IntegR project, takes geometric restrictions into account that make a structural realizability more likely. Within the current investigation, the maximum curvature of the SC bump is limited to 7/m to enable a feasible morphing spoiler structure. Details on the SC bump shape are provided by Goerttler et al. [6]. SCB1 and SC are exemplary shown in Fig. 2 for different crest positions x_{cr} and crest heights h_{cr}. Besides focusing on SCBs in combination with VC only in terms of shifting the buffet boundary to higher c_L values when the position and shape is restricted due to structural constraints, a combined SCB suitable for wave drag reduction and buffet onset delay is a major goal in SCB design. This approach of using a combined bump is motivated by the concept of using a single actuator to create a position-fixed SCB on a morphing spoiler as investigated e.g. in [7]. Therefore, a bump based on the SC shape but optimized for wave drag reduction by Goerttler et al. [6] is considered. Based on this aerodynamic bump shape and the corresponding aerodynamic forces, a structural design of an adaptive bump was conducted on a morphing spoiler with the process chain presented by Künnecke et al. [7]. The resulting bump shape of this structurally optimized morphing spoiler, further called *Drag Reduction* (DR), is used to investigate whether VC can be used to utilize a bump shape optimized for drag reduction also for buffet onset delay. Within the investigations of Goerttler et al. [6], the range of the spoiler was increased upstream to the position of the rear spar. Hence, the DR bump ranges from $65\% \leq x/c \leq 85\%$ with $x_{cr}/c = 77.5\%$ and $h_{cr}/c = 0.32\%$, see Fig. 2.

3 Buffet Onset Delay by Application of Variable Camber

The capabilities of VC to increase the efficiency of SCBs located on the spoiler of the HLFC wing section are presented in the following. First, the SCB performance without VC is briefly presented. It is followed by a detailed analysis of the impact of upward directed trailing edge deflections on the SCB performance in terms of buffet onset delay and the corresponding aerodynamic mechanisms.

3.1 SCB Performance Without VC

Waldmann et al. [17] performed an extensive study on different crest positions and bump heights of two selected SCB shapes for buffet onset delay at the same

wing section of the XRF1-HLFC wing. They show, that the geometric restriction of the bump to be located on the spoiler geometry limits the capability of the SCB in terms of increasing the lift coefficient of buffet onset. Within the spatial constraints it is shown, that both, SCB1 and SC have the highest potential for buffet onset delay for crest positions $x_{cr}/c \approx 83.5\%$ to 84%, very close to the rear end of the spoiler, and high crest heigths of $h_{cr}/c \approx 7\%$. These high bumps with far downstream located crest positions are hard to realize on an aircraft structure due to the high curvatures and the necessary prebend of the spoiler to hold the spoiler's trailing edge against the aerodynamic loads down on the flap. Based on the findings of Waldmann et al. [17], the parameter range of SCB1 and SC bump shapes used for the subsequent VC investigations is selected. While the bump position is fixed to the spoiler ($70\% \leq x/c \leq 85\%$), the following crest positions and crest heights are considered: $x_{cr} = [78, 80, 82, 83]\%c$, $h_{cr} = [0.2, 0.4, 0.6]\%c$. The increase in lift coefficient c_{L_b} at which buffet occurs at the current configuration compared to the buffet $c_{L_{b,clean}}$ of the clean airfoil, $\Delta c_L = \frac{c_{L_b} - c_{L_{b,clean}}}{c_{L_{b,clean}}}$ is used as a measure of bump efficiency on buffet onset delay. Figure 3 displays Δc_L for the selected SCB1 and SC bumps as well as the DR bump without VC. A shift of c_{L_b} up to 9% is possible for the most downstream crest position but hard to realize from a structural point of view due to the aforementioned necessary prebend. Shifting the bumps crest position further upstream decreases Δc_L significantly with even a negative impact on the buffet c_L at $x_{cr}/c = 78\%$. The structurally designed drag reduction (DR) bump shows the lowest Δc_L and is accordingly not applicable to buffet onset delay. The unfavorable position of the bump crest compared to the shock at the clean airfoil leads to the poor buffet onset delay performance of the SCBs at the more upstream positions, see [17]. Hence, for both, structurally realizable SCB1/SC bump shapes and the DR bump applied for buffet onset delay, the position of the shock has to be shifted further upstream. In the following, this is realized by deflecting the trailing edge flap, which alters the camber of the airfoil.
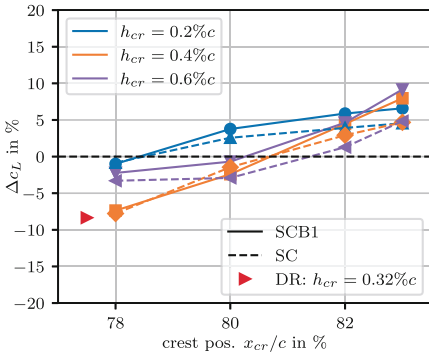

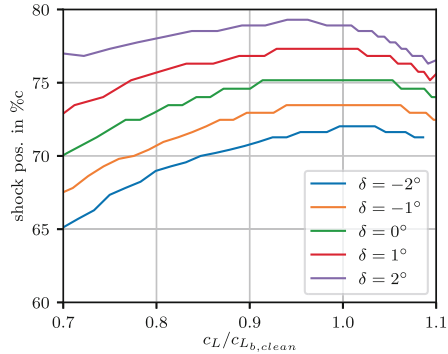**Fig. 3.** Buffet onset delay of different bumps without VC

Fig. 4. Shock position for different flap angles (clean airfoil)

3.2 Effect of VC on the Efficiency of SCBs for Buffet Onset Delay

First, the influence of different flap deflections δ on the shock position on the upper side of the clean airfoil without SCBs is evaluated in Fig. 4 in the relevant lift region close to the buffet c_{L_b} of the clean airfoil. Consistent with the results of Werner on a NLF wing [18], a downward directed flap deflection ($\delta > 0°$) leads to a downstream movement of the shock, while an upward flap deflection ($\delta < 0°$) shifts the shock towards the leading edge. As pointed out in Sect. 3.1, the shock needs to be shifted further upstream due to the structural constraints. Hence, only upward directed flap deflections with $-2° \leq \delta < 0°$ are applied to the SCBs shown in Fig. 3 to increase the efficiency of the SCBs for buffet onset delay. This allows a reliable statement about the potential and limits of VC at an acceptable number of simulations. Figure 5 shows the impact of the selected flap angles on the buffet performance of the SCB1 (Fig. 5a) and SC/DR bumps (Fig. 5b). The effect of VC on the buffet c_L of the clean airfoil is plotted as reference. VC is capable of increasing c_{L_b} up to 4% on the investigated HLFC wing section even without a SCB. Combining VC with SCBs, the buffet boundary can be shifted to higher c_L values for a wide parameter range of x_{cr} and h_{cr} for both, SCB1 and SC bump shapes. As is the case without VC, the aerodynamically optimized bump shape SCB1 has a slightly higher potential in increasing c_{L_b} (up to $\Delta c_L = 19.5\%$) than the SC bump design (up to $\Delta c_L = 14.8\%$), which focuses on structural feasibility. The highest Δc_L is achieved with $x_{cr}/c = 83\%$ and $h_{cr}/c = 0.6\%$. The clean airfoil as well as some bump shapes (e.g. SC with $x_{cr}/c = 83\%$ and $h_{cr}/c = 0.2\%$) reveal, that the potential of VC is limited, which is discussed in detail in Sect. 3.3. Another key finding from Fig. 5b is, that VC enables the use of a SCB optimized for wave drag reduction, with a shape that is structurally sized, for buffet onset delay. Δc_L can be raised by 14.9% up to $\Delta c_L = 6.6\%$. The trend of the curve shows, that higher flap deflection might lead to even higher Δc_L.
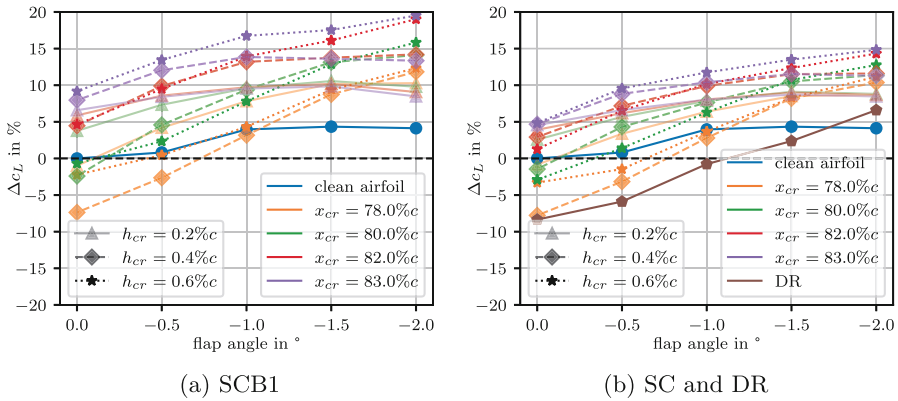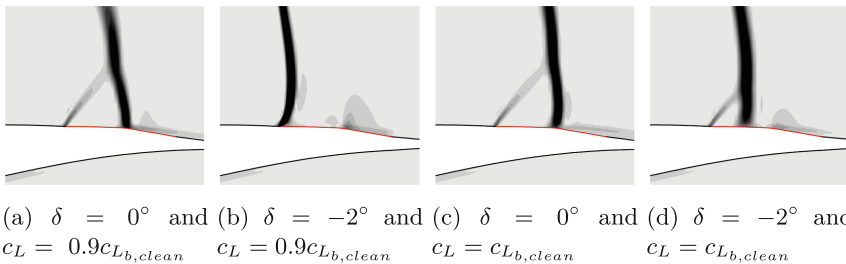

(a) SCB1

(b) SC and DR

Fig. 5. Buffet onset delay achievable with VC

### 3.3   Specific Analysis of Selected Bumps

Within this section, the aerodynamic effects leading to the increase in Δc_L when VC is applied are analyzed. Since the mechanisms are comparable for SCB1, SC and DR shape, only SC is considered within this section.

First, the SC bump with $x_{cr}/c = 78\%$ and $h_{cr}/c = 0.4\%$ at $\delta = 0°$ and $\delta = -2°$ is studied in more detail. Without VC, this bump has the most negative impact on the buffet c_L with $\Delta c_L = -7.8\%$, see Fig. 5b. With increasing upward directed flap deflection, c_{L_b} can be shifted up to $\Delta c_L = 11.6\%$. Figure 6 shows the density gradient for both cases at $c_L/c_{L_{b,clean}} = 90\%$ (Fig. 6a and 6b) and at $c_L = c_{L_{b,clean}}$ (Fig. 6c and 6d). Comparing the shock structures at $c_L/c_{L_{b,clean}} = 90\%$ it can be observed that without flap deflection (Fig. 6a) a λ-shaped shock structure develops. The first, weaker shock is fixed to the spoiler hinge due to the abrupt contour change. While there is no separation at $c_L/c_{L_{b,clean}} = 90\%$, shock induced separation extends over $\approx 10\%c$ at $c_{L_{b,clean}}$. Since the main shock is located at the bump crest, the bump is not capable of reattaching the separation within the extend of the bump, leading to an early shock oscillation as described in Sect. 1. With a flap deflection of $-2°$ at $c_L/c_{L_{b,clean}} = 90\%$ (Fig. 6b), there is only a single shock located at the spoiler hinge, which clearly shows, that VC is capable of shifting the shock position upstream even with a SCB. At higher c_L (Fig. 6d) a small λ-shaped shock structure develops but the main shock still remains further upstream than the bump crest. Due to the bump shape, the flow is accelerated between the shock and the bump crest, which effectively suppresses flow separation and accordingly delays buffet onset to higher c_L.

This effect can be seen in detail when looking at the pressure coefficient (c_p) and skin friction coefficient (c_f) distribution in the bump region for different bump heights at $c_{L_{b,clean}}$ (Fig. 7). The selected bump is the best performing SC bump ($x_{cr}/c = 83\%$, $h_{cr}/c = 0.6\%$) and its lower counterpart ($h_{cr}/c = 0.2\%$). Both are able to raise c_{L_b} with and without VC but the higher bump crest significantly increases the effectiveness of VC for buffet onset delay compared to the lower bump. The clean airfoil without bump and VC is plotted as reference. While the clean airfoil shows a significant shock induced separation region ($c_{f,x} < 0$), the $h_{cr}/c = 0.2\%$ bump without VC leads to a fast reattachment

(a) $\delta = 0°$ and (b) $\delta = -2°$ and (c) $\delta = 0°$ and (d) $\delta = -2°$ and
$c_L = 0.9c_{L_{b,clean}}$ $c_L = 0.9c_{L_{b,clean}}$ $c_L = c_{L_{b,clean}}$ $c_L = c_{L_{b,clean}}$

Fig. 6. Numerical Schlieren (SC: $h_{cr} = 0.4\%c$, $x_{cr} = 78\%c$), bump marked in red
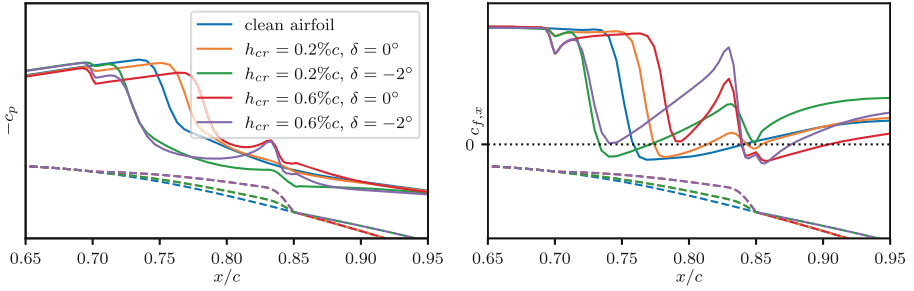
Fig. 7. c_p and $c_{f,x}$ on the suction side at $c_L = c_{L_b}$ of the clean airfoil for different SC bumps ($x_{cr} = 83\%c$) with and without VC. Dashed lines: Bump contour
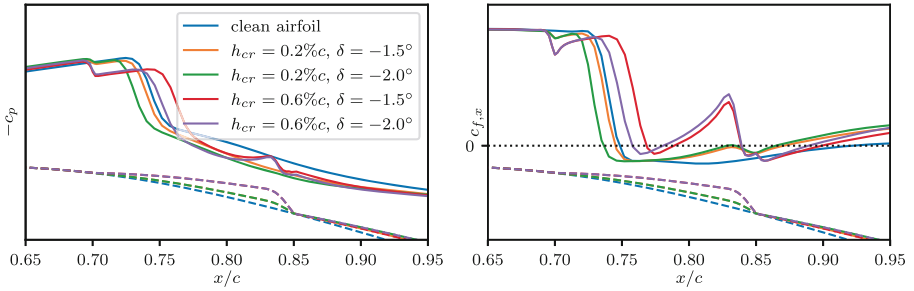
Fig. 8. c_p and $c_{f,x}$ on the suction side. $c_L = c_{L_b}$ of the SC bump with $h_{cr} = 0.2\%c$, $x_{cr} = 83\%c$, $\delta = -1.5°$. All SC bumps $x_{cr} = 83\%c$. Dashed lines: Bump contour

of the flow on the uprising bump flank, which delays the shock oscillation. The $h_{cr}/c = 0.6\%$ bump is even capable of completely suppressing the shock induced separation but leads to a separation region downstream of the bump crest due to the high curvature. A flap angle of $-2°$ shifts the main shock further upstream. This significantly increases the buffet onset delay. Even though the shock induced separation remains nearly unaffected for the shown c_L, the extend of the separation region downstream of the bump crest is considerably reduced or completely suppressed by the flap deflection.

Further analysis on the mechanisms of VC can be done when comparing $\delta = -1.5°$ with $\delta = -2°$ for the aforementioned bumps at a higher c_L. Figure 8 shows c_p and c_f distributions at the buffet c_L of the $x_{cr}/c = 83\%$, $h_{cr}/c = 0.2\%$, $\delta = -1.5°$ bump. While Δc_L of the SC bump with $h_{cr}/c = 0.6\%$ increases when the flap is further deflected upwards from $\delta = -1.5°$ to $\delta = -2°$, it leads to a slight reduction in Δc_L for $h_{cr}/c = 0.2\%$. For both bump heights, the shock is shifted upstream due to the increased flap deflection with a shock induced separation occurring at all cases. With $h_{cr}/c = 0.2\%c$, the higher flap deflection shifts the shock itself, and correspondingly the starting point of the shock induced separation to a more upstream position. This increases the total size of the separation region since the earlier reattachment of the flow downstream of

the bump due to the higher flap deflection is less pronounced than the shift in shock position. The bump crest itself is not high enough to ensure a relevant reattachment of the flow on the bump. Hence, c_{L_b} cannot be shifted to a higher c_L when increasing the flap deflection from $\delta = -1.5°$ to $\delta = -2°$. A different situation occurs when the bump height is increased to $h_{cr}/c = 0.6\%$. Due to the high curvature at the bump crest, the flow is accelerated upstream from the crest, which leads to a fast reattachment of the flow upstream the bump crest position with a comparable chordwise extend of the shock induced separation region for both flap angles. The flow acceleration is also visible in the peak in the c_p distribution at the bump crest (see Fig. 8). The flow separates again downstream of the bump crest position, where the higher flap angle of $\delta = -2°$ leads to an earlier reattachment. Hence, for the higher bump crest, c_{L_b} can still be shifted to higher c_L when increasing the flap deflection from $\delta = -1.5°$ to $\delta = -2°$, which is not possible for the lower bump crest.

4   Conclusion

The analyses above have shown that VC can be used to increase the effectiveness of SCBs integrated into the spoiler on a HLFC wing section in terms of buffet onset delay. Without VC, the highest achievable Δc_L is 9% within the selected parameter range. However, this is only possible when the crest position is located close to the rear end of the bump, which impedes a structural realization. Hence, more upstream located crest positions are being pursued. Since this decreases Δc_L due to the unfavorable position of the bump crest relative to the shock, an upward directed flap deflection can be used to increase c_{L_b}. With moderate flap angles up to $\delta = -2°$, an increase in c_{L_b} up to 19.5% compared to the clean airfoil can be achieved. Even for the most upstream located bump crest positions, which fulfill the structural realization requirements, an increase in c_{L_b} of about 10% is possible. This demonstrates, that VC is applicable for different bump shapes over a wide range of bump crest positions and bump heights. In addition, VC enables the use of a common bump shape for wave drag reduction and buffet onset delay. This reduces the difficulty in designing multifunctional bumps, and simplifies system integration and complexity. VC is capable of shifting the shock position to more favorable positions relative to the bump. Hence, shock induced flow separation can be reduced, increasing the effectiveness of the SCB. Furthermore, the upward directed flap deflection diminishes the flow separation occurring downstream of the bump crest. Both effects shift buffet onset to higher c_L and extend the flight envelope to higher Mach numbers and angles of attack.

References

1. Ashill, P., Fulker, J., Shires, A.: A novel technique for controlling shock strength of laminar flow airfoil sections. Technical report, DGLR, Part 6(92-01-022), pp. 175-183 (1992)
2. Birkemeyer, J., Rosemann, H., Stanewsky, E.: Shock control on a swept wing. Aerosp. Sci. Technol. **4**(3), 147–156 (2000). https://doi.org/10.1016/S1270-9638(00)00128-0
3. Bruce, P.J.K., Colliss, S.P.: Review of research into shock control bumps. Shock Waves **25**(5), 451–471 (2015). https://doi.org/10.1007/s00193-014-0533-4
4. Despré, C., Caruana, D., Mignosi, A., Reberga, O., Corrège, M.: Buffet active control-experimental and numerical results. Technical report, ONERA (FRANCE) (2001)
5. Giannelis, N.F., Vio, G.A., Levinski, O.: A review of recent developments in the understanding of transonic shock buffet. Prog. Aerosp. Sci. **92**, 39–84 (2017). https://doi.org/10.1016/j.paerosci.2017.05.004
6. Goerttler, A., Künnecke, S.C., Sabater, C.: Aerodynamic design of shock control bumps considering structural constraints. In: Dillmann, A., Heller, G., Krämer, E., Wagner, C., Weiss, J. (eds.) New Results in Numerical and Experimental Fluid Mechanics XIV. STAB/DGLR Symposium 2022. NNFM, vol. 154. Springer, Cham (2024). https://doi.org/10.1007/978-3-031-40482-5_63
7. Künnecke, S.C., Goerttler, A., Vasista, S., Riemenschneider, J.: Strukturkonzept eines vorgebogenen morphenden Spoilers zur adaptiven transsonischen Stosskontrolle. 4SmartS conference proceedings, Braunschweig, Germany (2022)
8. Lawson, S., Greenwell, D., Quinn, M.K.: Characterisation of buffet on a civil aircraft wing. In: 54th AIAA Aerospace Sciences Meeting. San Diego, USA (2016). https://doi.org/10.2514/6.2016-1309
9. Lee, B.H.K.: Effects of trailing-edge flap on buffet characteristics of a supercritical airfoil. J. Aircr. **29**(1), 93–100 (1992)
10. Mayer, R., Lutz, T., Krämer, E., Dandois, J.: Control of transonic buffet by shock control bumps on wing-body configuration. J. Aircr. **56**(2), 556–568 (2019). https://doi.org/10.2514/1.C034969
11. Mayer, R., Lutz, T., Krämer, E.: Numerical study on the ability of shock control bumps for buffet control. AIAA J. **56**(5), 1978–1987 (2018). https://doi.org/10.2514/1.J056737
12. Obert, E., Slingerland, R., Leusink, D.J.W., van den Berg, T., Koning, J.H., van Tooren, M.J.L.: Aerodynamic Design of Transport Aircraft. Ios Press, Amsterdam (2009)
13. Richter, K., Strohmeyer, D., Rosemann, H.: Numerische Untersuchungen an transsonischen Profilen mit flexibler Hinterkante und Konturbeule. Deutscher Luft- und Raumfahrtkongress 2000, Leipzig, Germany (2000)
14. Rossow, C.C., Kroll, N., Schwamborn, D.: The MEGAFLOW Project – Numerical Flow Simulation for Aircraft. In: Di Bucchianico, A., Mattheij, R., Peletier, M. (eds.) Progress in Industrial Mathematics at ECMI 2004. Mathematics in Industry, vol. 8, pp. 3–33. Springer, Berlin, Heidelberg (2006). https://doi.org/10.1007/3-540-28073-1_1
15. Sommerer, A., Lutz, T., Wagner, S.: Design of adaptive transonic airfoils by means of numerical optimisation. In: European Congress on Computational Methods in Applied Sciences and Engineering, Barcelona, Spain (2000)

16. Streit, T., Kruse, M., Kilian, T., v. Geyr, J., Petropoulos, I.: Aerodynamic design and analysis of HLFC wings within the European Project HLFC-WIN. In: 33rd Congress of the International Council of the Aeronautical Sciences (ICAS), Stockholm, Sweden (2022)
17. Waldmann, A., Müller, J., Goerttler, A., Lutz, T.: Shock control bumps for buffet onset delay on sections of a wing with hybrid laminar flow control. In: Dillmann, A., Heller, G., Krämer, E., Wagner, C., Weiss, J. (eds.) New Results in Numerical and Experimental Fluid Mechanics XIV. STAB/DGLR Symposium 2022. NNFM, vol. 154. Springer, Cham (2024). https://doi.org/10.1007/978-3-031-40482-5_65
18. Werner, M.: Application of an adaptive shock control bump for drag reduction on a variable camber NLF wing. In: 2018 AIAA Aerospace Sciences Meeting. American Institute of Aeronautics and Astronautics, Kissimmee, USA (2018). https://doi.org/10.2514/6.2018-0789